
Volume 256, Issue 14 1 May 2010 ISSN 0169-4332
ELSEVIER
applied
surface science
A journal devoted to applied physics
and chemistry of surfaces and interfaces
Editors
F.H.P.M. Habraken, Utrecht, The Netherlands
H. Kobayashi, Osaka, Japan
R.R.L. Opila, Newark, DE, USA
H. Rudolph, Utrecht, The Netherlands
P. Schaaf, Ilmenau, Germany
S. Suzer, Ankara, Turkey
Volume 256, Issue 14, pp. 4411–4762
1 May 2010
Available online at www.sciencedirect.com
ScienceDirect

Applied Surface Science 256 (2010) 4734–4737

Contents lists available at ScienceDirect

Applied Surface Science

journal homepage: www.elsevier.com/locate/apsusc

Thermal stability of CdZnO thin films grown by molecular-beam epitaxy

L. Li, Z. Yang, Z. Zuo, J.H. Lim, J.L. Liu*

Quantum Structures Laboratory, Department of Electrical Engineering, University of California, Riverside, CA 92521, USA

ARTICLE INFO

Article history:
Received 12 July 2009
Received in revised form 26 February 2010
Accepted 27 February 2010
Available online 18 March 2010

PACS:
78.55.Et
68.60.Dv
81.15.Hi
81.40.Ef
81.40.Tv

Keywords:
ZnO
Thermal stability
Molecular-beam epitaxy
II–VI semiconductors
X-ray diffraction
Photoluminescence

ABSTRACT

CdZnO thin films with near-band-edge (NBE) photoluminescence (PL) emission from 2.39 eV to 2.74 eV were grown by plasma-assisted molecular-beam epitaxy on *c*-plane sapphire substrates with 800 °C in situ annealing. CdZnO thin films evolve from pure wurtzite (wz) structure, to mixture of wz and rock-salt (rs) structures confirmed by X-ray diffraction studies. Rapid-thermo-annealing (RTA) was performed on in situ annealed CdZnO samples. Pure wz CdZnO shows insignificant NBE PL peak shift after RTA, while mixture structure CdZnO shows evident blue shifts due to phase change after annealing, indicating the rs phase CdZnO changes to wz phase CdZnO during RTA process.

1. Introduction

ZnO attracts considerable attentions for ultra-violet/blue light emitting diodes and laser diodes (LDs) due to its direct bandgap of 3.3 eV and large exciton binding energy of 60 meV at room temperature. The bandgap of ZnO can be made smaller by alloying Cd into ZnO [1–6] for potential visible light emitting device applications, such as green LDs. The thermal stability of CdZnO is an important issue for future reliable device application [7,8]. Due to the different crystal structures between wurtzite (*wz*) ZnO and rock-salt (*rs*) CdO, phase separation from *wz* to *rs* tends to happen in CdZnO, especially when large amount of Cd is alloyed into ZnO [4,9,10]. However, phase segregation and thermal stability studies of CdZnO have seldom been reported so far, especially on how the optical properties change after annealing. Since in situ annealing is an indispensable process for dopant activation [11–14], while RTA under nitrogen ambient is normally used for device contact formation [15–18] for ZnO based materials, we studied and reported the rapid thermal annealing effect on molecular-beam epitaxy (MBE) grown CdZnO thin films in this paper.

2. Experiment

CdZnO thin films were grown by plasma-assisted MBE on *c*-plane sapphire substrates. Elemental Zn (6N) and Cd (6N) heated by effusion cells were used as zinc and cadmium sources. Oxygen (5N) plasma generated by a radiofrequency plasma generator was used as the oxygen source. The samples were grown at very low growth temperatures (below 200 °C) to achieve large Cd incorporation. A thin ZnO buffer layer (10–20 nm) was first grown on substrate before CdZnO growth for each sample. These CdZnO samples were in situ vacuum-annealed in the chamber at 800 °C for 5 min after growth. Cd composition was controlled by tuning the ratio of Zn and Cd flux. Cd composition was measured by energy-dispersive X-ray spectroscopy (EDS). Room temperature (RT) PL measurements were carried out using a home-built PL system, with a 325-nm He–Cd laser as excitation source and a photomultiplier tube behind the monochrometer as detector. RTA was then carried out at 800 °C in nitrogen ambient for 1 min on the CdZnO samples. X-ray diffraction (XRD) was performed in θ–2θ geometry with a 0.1° resolution. To avoid the possible effect of non-uniformity of the

---

* Corresponding author. Tel.: +1 951 8277131; fax: +1 951 8272425.
E-mail address: jianlin@ee.ucr.edu (J.L. Liu).

0169-4332/$ – see front matter © 2010 Elsevier B.V. All rights reserved.
doi:10.1016/j.apsusc.2010.02.083

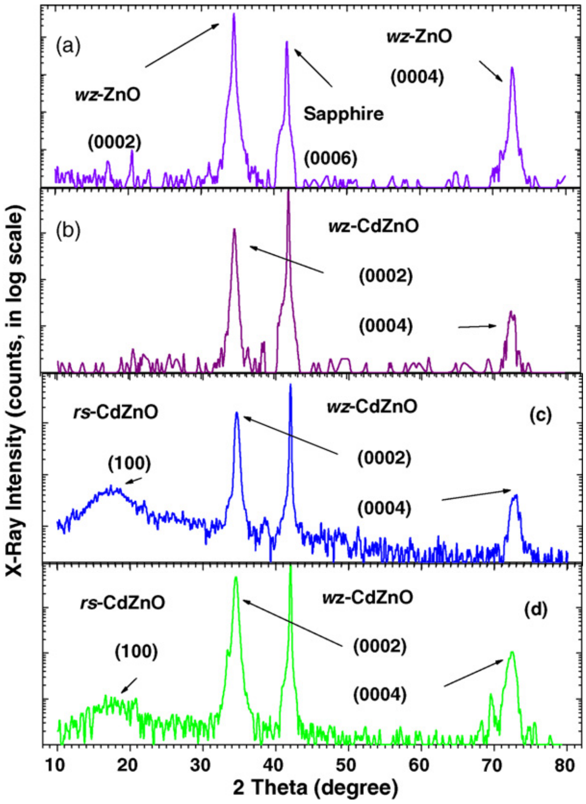

Fig. 1. XRD patterns of ZnO sample A (a) and CdZnO B–D [(b)–(d)]. The CdZnO samples evolve from pure wurtzite structure (B) to mixture of wurtzite and rock-salt structures (C and D) with increasing Cd composition.

samples on the spectra, PL and XRD measurements of the samples before and after RTA were carried out on less than 5 mm × 5 mm area of each sample.

3. Results and discussions

Fig. 1(a) and (b)–(d) show the XRD patterns of undoped ZnO sample A, and CdZnO samples B–D respectively. Samples A and B show only *wz*-ZnO/*wz*-CdZnO (0 0 0 2) and (0 0 0 4) peaks at $2\theta = 34.5^\circ$ and 72.5° as shown in Fig. 1(a) and (b), indicating the pure *wz* structure. As Cd concentration is increased monotonously, samples C and D become mixture of *wz* and *rs* structures as shown in Fig. 1(c) and (d). Besides the *wz*-CdZnO (0 0 0 2) and (0 0 0 4) peaks, a broad *rs*-CdZnO (1 0 0) peak [19,20] at $2\theta = 17.5^\circ$ is also observed, indicating the emergence of phase segregation in samples C and D, although the *wz* structure still dominates as sharper peaks. The intensity of *rs*-CdZnO (1 0 0) peak does not show significant change with increasing Cd concentration. The broad *rs*-CdZnO (1 0 0) peak is possibly due to the very low crystallinity of the *rs* phase in the CdZnO samples. In the XRD patterns, substrate signals of sapphire (0 0 0 6) peaks at $2\theta = 42.0^\circ$ are shown in all samples A–D. The crystal structures of the samples are summarized in Table 1. The Cd concentrations (x) of $Cd_xZn_{1-x}O$ samples B–D are also listed in Table 1, which show 0.05, 0.08 and 0.13, respectively.

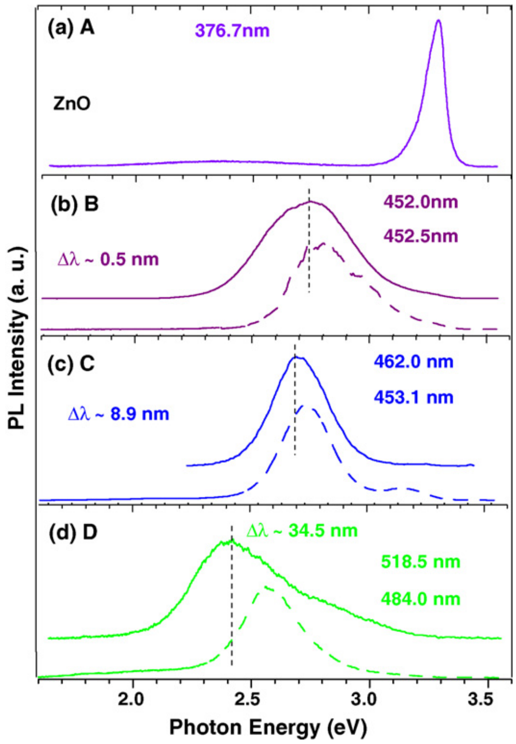

Fig. 2. Room-temperature PL spectra before (solid lines) and after (dashed lines) RTA of CdZnO samples B–D in (b)–(d). The upper and lower wavelength values in (b)–(d) show the RT PL peak positions before and after RTA. The blue shift values are shown as Δλ. Room-temperature PL spectra of ZnO sample are shown in (a) as reference.

Samples B–D were subject to the following experiments to investigate the annealing effect on the CdZnO. Firstly, RT PL measurements were performed on the as-grown samples B–D [solid lines shown in Fig. 2(b)–(d)]. Table 1 summarizes the CdZnO samples B–D with RT NBE PL positions covering from 2.74 eV to 2.39 eV, corresponding from violet to green in the visible region. The room-temperature NBE PL energies are assumed to be the bandgap energies of each sample. Then, the CdZnO samples were rapid thermal annealed at 800 °C for 1 min. Finally, the RT PLs were carried out on the annealed samples. The dashed lines in Fig. 2(b)–(d) show the RT PL spectra of CdZnO samples B-D after RTA. In pure *wz*-CdZnO sample B, the NBE RT PL peak position shifted from 452.0 nm (2.743 eV) to 452.5 nm (2.740 eV) after RTA as shown in Fig. 2(b). The blue shift is only 0.5 nm, which is comparable to the resolution of the PL measurements. However, the RT NBE PL peaks of the mixture structural CdZnO samples C and D shift from 462.0 nm (2.684 eV) to 453.1 nm (2.737 eV), and from 518.5 nm (2.392 eV) to 484.0 nm (2.562 eV) after RTA, respectively. The blue shifts of 8.9 and 34.5 nm are observed, respectively.

To find out the reason of bandgap change after RTA, secondary ion mass spectroscopy (SIMS), EDS and XRD were carried out on

Table 1
Crystal structure, bandgap E_g, film thickness and Cd concentration x in the $Cd_xZn_{1-x}O$ samples.

Sample no.	Description	Crystal structure[a]	Bandgap E_g[b] (eV)	Thickness (nm)	Cd concentration x
A	ZnO	*wz*	3.29	260	0
B	CdZnO	*wz*	2.74	200	0.05
C	CdZnO	*wz* and *rs*	2.68	150	0.08
D	CdZnO	*wz* and *rs*	2.39	200	0.13

[a] wz and rs represent wurtzite and rock-salt structures, respectively.

[b] RT NBE PL peak positions of the samples before RTA are approximately used for E_g of the samples.

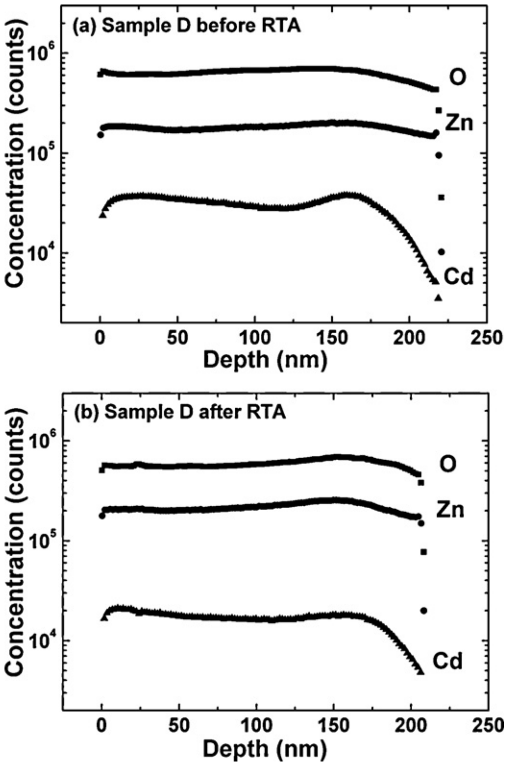

Fig. 3. SIMS spectra of a typical CdZnO (sample D) (a) before and (b) after RTA.

the samples after RTA. Fig. 3(a) and (b) shows the SIMS spectra of mixture of *wz* and *rs* structure CdZnO sample D before and after RTA, respectively. Comparing Fig. 3(a) with Fig. 3(b), it is found that sample D exhibits similar Cd distribution profile and signal strength before and after RTA. EDS measurements after RTA show Cd concentration *x* of samples B–D to be 0.04, 0.07 and 0.12 respectively, which are slightly lower than, but close to the values measured before RTA as shown in Table 1.

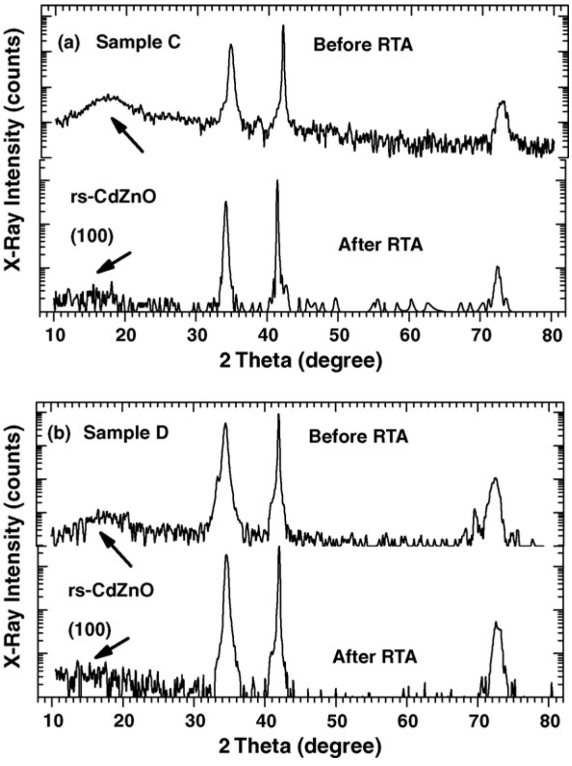

Fig. 4. XRD spectra of CdZnO sample C (a) and D (b) before (upper curve) and after (lower curve) RTA. The vertical axis is plotted in log scale.

Fig. 4 shows the XRD spectra of sample C and sample D before and after RTA. The broad *rs*-CdZnO (1 0 0) peak as also shown in Fig. 1(c) and (d) is weakened after RTA, indicating that the mixture of *wz* and *rs* structure is changed to pure *wz* structure. With more CdZnO changing from *rs* phase to *wz* phase, the bandgap increases. It may be due to the fact that the bandgap of *rs*-CdZnO is smaller than *wz*-CdZnO with the same Cd composition. Alternatively, less band-tail states are expected due to less alloy disordering from *rs*-/*wz*-CdZnO mixture to pure *wz*-CdZnO as a result of RTA annealing. While the experimental results are reasonable to explain the phase change from *rs* to *wz* during annealing, we speculate that the in situ annealing at 800 °C for 5 min is not long enough to convert all *rs* phases formed in the film during the extremely low growth temperature below 200 °C to *wz* phases, and additional RTA annealing at 800 °C together with fast temperature ramping processes is needed to obtain more stable *wz*-CdZnO phases.

4. Summary

CdZnO thin films with bandgap covering from violet to blue were grown using plasma-assisted molecular-beam epitaxy. With more Cd alloyed into the thin films, the CdZnO samples evolve from single *wz* structure, to a mixture of *wz* and *rs* structures. The *wz*-CdZnO shows robust thermal stability during RTA process, however, the mixture structural CdZnO shows weak thermal stability during RTA process, with noticeable NBE RT PL peak blue shift after RTA. The origin of the blue shift might be contributed by the phase change during the annealing process. The approach to achieve thermo-robust CdZnO is to push the *wz* and *rs* phase separation point towards larger Cd concentration direction, which is a critical issue for the device application of CdZnO materials.

Acknowledgements

This work was supported by UC Micro/ZN Technology Inc. and ARO-YIP under grant number W911NF-08-1-0432.

References

[1] T. Makino, Y. Segawa, M. Kawasaki, A. Ohtomo, R. Shiroki, K. Tamura, T. Yasuda, H. Koinuma, Appl. Phys. Lett. 78 (2001) 1237.
[2] Ü. Özgür, Ya.I. Alivov, C. Liu, A. Teke, M.A. Reshchikov, S. Doğan, V. Avrutin, S.-J. Cho, H. Morkoç, J. Appl. Phys. 98 (2005) 041301, (And reference therein).
[3] S. Shigemori, A. Nakamura, J. Ishihara, T. Aoki, J. Temmyo, Jpn. J. Appl. Phys. 43 (2004) L1088.
[4] J. Ishihara, A. Nakamura, S. Shigemori, T. Aoki, J. Temmyo, Appl. Phys. Lett. 89 (2006) 091914.
[5] A.V. Osinsky, J.W. Dong, J.Q. Xie, B. Hertog, A.M. Dabiran, P.P. Chow, S.J. Pearton, D.P. Norton, D.C. Look, W. Schoenfeld, O. Lopatiuk, L. Chernyak, M. Cheung, A.N. Cartwright, M. Gerhold, Mater. Res. Soc. Symp. Proc. 892 (2006), FF18-01-EE09-01.
[6] S. Sadofev, S. Blumstengel, J. Cui, J. Puls, S. Rogaschewski, P. Schäfer, F. Henneberger, Appl. Phys. Lett. 89 (2006) 201907.
[7] A.V. Thompson, C. Boutwell, J.W. Mares, W.V. Schoenfeld, A. Osinsky, B. Hertog, J.Q. Xie, S.J. Pearton, D.P. Norton, Appl. Phys. Lett. 91 (2007) 201921.
[8] S. Sadofev, S. Kalusniak, J. Puls, P. Schäfer, S. Blumstengel, F. Henneberger, Appl. Phys. Lett. 91 (2007) 231103.
[9] Y.Z. Zhu, G.D. Chen, H. Ye, A. Walsh, C.Y. Moon, S.-H. Wei, Phys. Rev. B 77 (2008) 245209.
[10] K. Sakurai, T. Takagi, T. Kubo, D. Kajita, T. Tanabe, H. Takasu, S. Fujita, S. Fujita, J. Cryst. Growth 237–239 (2002) 514.
[11] F.X. Xiu, Z. Yang, L.J. Mandalapu, D.T. Zhao, J.L. Liu, W.P. Beyermann, Appl. Phys. Lett. 87 (2005) 152101.
[12] F.X. Xiu, Z. Yang, L.J. Mandalapu, D.T. Zhao, J.L. Liu, Appl. Phys. Lett. 87 (2005) 252102.
[13] F.X. Xiu, Z. Yang, L.J. Mandalapu, J.L. Liu, W.P. Beyermann, Appl. Phys. Lett. 88 (2006) 052106.
[14] F.X. Xiu, Z. Yang, L.J. Mandalapu, J.L. Liu, Appl. Phys. Lett. 88 (2006) 152116.

[15] L.J. Mandalapu, Z. Yang, F.X. Xiu, D.T. Zhao, J.L. Liu, Appl. Phys. Lett. 88 (2006) 092103.
[16] L.J. Mandalapu, Z. Yang, J.L. Liu, Appl. Phys. Lett. 90 (2007) 252103.
[17] L.J. Mandalapu, Z. Yang, S. Chu, J.L. Liu, Appl. Phys. Lett. 92 (2008) 122101.
[18] S. Chu, M. Olmedo, Z. Yang, J.Y. Kong, J.L. Liu, Appl. Phys. Lett. 93 (2008) 181106.
[19] H. Liu, H.K. Mao, M. Somayazulu, Y. Ding, Y. Meng, D. Häusermann, Phys. Rev. B 70 (2004) 094114.
[20] C. Alétru, G.N. Greaves, G. Sankar, J. Phys. Chem. B 103 (1999) 4147.